Asian Journal of Chemistry; Vol. 25, No. 13 (2013), 7365-7370

ASIAN JOURNAL OF CHEMISTRY

http://dx.doi.org/10.14233/ajchem.2013.14655

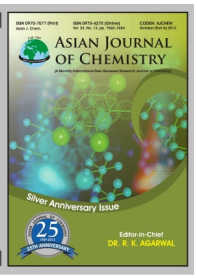

Electronic Structure and Related Properties of DNA-Molecular Light-Switch Complex $[Ru(bpy)_2(bopp)]^{2+}$

JUN LI[1,*], TI-FANG MIAO[2], SI-YAN LIAO[3] and KANG-CHENG ZHENG[3]

[1]Department of Chemistry, Guangdong University of Education, Guangzhou 510303, P.R. China
[2]College of Chemistry and Materials Science, Huaibei Normal University, Huaibei 235000, P.R. China
[3]Key Laboratory of Bioinorganic and Synthetic Chemistry of Ministry of Education; School of Chemistry and Chemical Engineering, Sun Yat-Sen University, Guangzhou 510275, P.R. China

*Corresponding author: E-mail: lijun61@hotmail.com

(*Received*: 8 October 2012; *Accepted*: 28 June 2013) AJC-13709

The electronic structure and related properties of a novel DNA-molecular light-switch complex $[Ru(bpy)_2(bopp)]^{2+}$ (bpy = 2,2'-bipyridine; bopp = 2-benzoxazolyl-pyrazino[2,3-f][1,10]phenanthroline) (**1**) has been investigated applying DFT/TDDFT (density functional theory and time-dependent DFT) methods. The comparison with well-accepted DNA-molecular light-switch complex $[Ru(bpy)_2(dppz)]^{2+}$ (dppz = dipyrido-[3,2-a:2',3'-c]phenazine) (**2**), the important geometric and electronic structural characteristics of complex **1** which can be expected to be an excellent DNA-molecular light-switch complex, were theoretically revealed. Moreover, it is further shown that such geometric and electronic structural characteristics can be obtained *via* introducing some heteroatoms (N and O atoms) with stronger electronegativity into the ring skeleton of main ligand. In particular, the ^{1}MLCT spectra of complex **1** in aqueous solution were calculated and simulated by the TDDFT method in a satisfying agreement with experimental results. Based on the electric structure, the experimental three main UV-visible bands (~448, ~363 and ~284 nm) were theoretically explained in detail and some regularities regarding strong absorption spectral bands were also presented. These theoretical results help to designing novel DNA-molecular light-switch complexes and understanding the spectral properties.

Key Words: Ru(II) complex, Light switch, DNA-Binding, Density functional theory, Time-dependent density functional theory.

INTRODUCTION

Over the past decade, it has been substantial interest in the DNA binding properties of many Ru(II) complexes, in the hope of developing novel probes of DNA structure or new molecular light-switches[1-3]. Since the well-known Ru(II) polypyridyl complexes $[Ru(phen)_2(dppz)]^{2+}$ and $[Ru(bpy)_2(dppz)]^{2+}$ were found to be excellent DNA molecular light-switches, which exhibit a negligible background emission in water but exhibit an intense luminescence in the presence of double strand DNA[4-6]. Although the DNA-molecular light-switch mechanism is still a complicated subject, it is well-accepted that the marked luminescence enhancement for DNA-molecular light-switch complexes $[Ru(L)_2(dppz)]^{2+}$ (L = phen, bpy) can owe to their main ligand (dppz) binding to the DNA-base-pairs in intercalative mode, because the intercalative ligand (dppz) of the complexes can be protected by the DNA from its interaction with solvent water molecules, resulting in an enormous increase in quantum yield. Moreover, it is also well-accepted that the luminescence of these complexes stems from a localized metal-to-ligand charge transfer (MLCT) transition. These properties are perturbed upon their binding to DNA, providing a sensitive handle for interactions[7-9]. Although a large number of Ru(II) polypyridyl complexes have synthesized and investigated, so far only few these complexes can be expected to be DNA-light-switches[10-14]. Recently, a structurally novel DNA-molecular light-switch complex $[Ru(bpy)_2(bopp)]^{2+}$ has been reported and many experimental studies for this complex have been performed[15,16]. However, a detailed theoretical study which reveals the DNA-light-switch essential from the geometric and electronic structures of the complex has not found yet. It is generally accepted that the excellent DNA-light-switch properties of the complex must depend on its geometric and electronic structures, especially the latter. Therefore, it is very significant to carry out the theoretical studies on the geometric and electronic structures, as well as the related properties, in order to reveal the essential that this novel complex can be a DNA-light-switch complex.

Besides the general density functional theory (DFT) method, the time dependent density functional theory

(TDDFT) method has been successfully used to calculate the electronic structures, electronic spectra as well as chemical reaction processes of many complexes[17-19]. Even though errors by using approximate exchange-correlation (XC) functionals and failures of TDDFT in describing excited states of the long-range charge transition systems have been reported, it can be solved by using approximate functionals corrected for long-range effects[20-26]. The absorption spectra of Ru(II) complexes are generally accurately reproduced by using TDDFT method and taking solvent effects into account[27,28]. Recently, we have reported some TDDFT studies on spectral properties of Ru(II) polypyridyl complexes. The computed results are in a good agreement with the experimental ones and thus provide good explanations and predictions for the experimental findings[29-33].

In this work, the theoretical studies on the geometric and electronic structures, as well as the related properties of a novel DNA-molecular light-switch complex $[Ru(bpy)_2(bopp)]^{2+}$ **1** were carried out applying DFT/TDDFT methods. *Via* the comparison with the well-accepted DNA-molecular light-switch complex $[Ru(bpy)_2(dppz)]^{2+}$ **2**, the geometric and electric structure-characteristics of complex **1** which can be expected to be an excellent DNA-molecular light-switch complex were revealed. In particular, the UV-visible absorption-spectral properties of $[Ru(bpy)_2(bopp)]^{2+}$ in aqueous solution were calculated, simulated and explained in a satisfying agreement with experimental results.

COMPUTATIONAL METHOD

Structural schematic diagram of the octahedral complex $[Ru(bpy)_2(bopp)]^{2+}$ **1** is shown in Fig. 1. The complex is formed from Ru(II) atom, one main ligand 2-benzoxazolyl-pyrazino-[2,3-f][1,10]phenanthroline (bopp) and two co-ligands 2,2′-bipyridine (bpy). First, the DFT calculations were carried out at the level of the B3LYP approach and the LanL2DZ basis set (ECP+DZ for Ru atom, D95 for other atoms)[34-36] using the Gaussian 03 program package (Revision D.01)[37]. The geometric optimization of the ground state of the complex in vacuo was all performed without symmetric constraint. Furthermore, the stable configuration of the complex was confirmed by frequency analysis, in which no imaginary frequency was found for each configuration at the energy minima. Then, two hundred singlet-excited-states in aqueous solution were calculated at the TDDFT method. The conductor-like polarizable continuum model (CPCM) was adapted in the calculations of solvent effect[38]. In addition, to distinctly and easily understand the UV-visible spectral properties, the stereo-contour graphs of some related frontier molecular orbitals of the complex $[Ru(bpy)_2(bopp)]^{2+}$ existing in aqueous solution, using the DFT/TDDFT method at the B3LYP/ LanL2DZ level, were also drawn with the Molden v4.2 program[39].

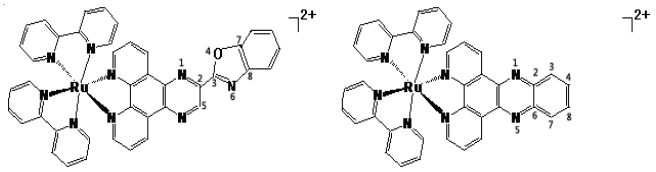

Fig. 1. Structure of $[Ru(bpy)_2(bopp)]^{2+}$ (**1**) and $[Ru(bpy)_2(dppz)]^{2+}$ (**2**)

RESULTS AND DISCUSSION

Main ligand effects on selected bond lengths and bond angles of the complexes: The report on the crystal structure of the novel complex $[Ru(bpy)_2(bopp)]^{2+}$ **1** has not been found yet, so the direct comparison between the computational results and the corresponding experimental data can not be performed. However, *via* comparing the computed values with the well-reported experimental ones for the parent complex $[Ru(bpy)_3]^{2+}$ (marked as **0**)[40] (Table-1), we can reasonably deduce that the results of the full geometry optimization computations by the DFT method should be reliable. The computational selected bond lengths, bond angles and dihedral angles of the novel complex $[Ru(bpy)_2(bopp)]^{2+}$ **1** and $[Ru(bpy)_2(dppz)]^{2+}$ **2** and $[Ru(bpy)_3]^{2+}$ **0** for comparison are shown in Table-1, from which we can see some important structural characteristics of complex **1** similar to the well-accepted DNA-light-switch complex **2** as follows: First, they have similar calculated enlarged coordination bond lengths, *i.e.*, Ru-N_m (**1**, 0.2111 nm) Ru-N_m(**2**, 0.2109 nm) > Ru-N_m(**0**, 0.2079 nm) and Ru-N_∞ (**1**, 0.2098 nm) Ru-N_∞(**2**, 0.2097 nm) > Ru-N_∞(**0**, 0.2079 nm). Second, the mean bond lengths of ring skeleton of their main ligands have similar slightly enlarged, *i.e.*, C-C$(N)_m$ (1, 0.1401 nm) and C-C$(N)_m$ (2, 0.1403 nm) > C-C$(N)_m$ (0, 0.1400 nm). These two points can be attributed to the greatly enlarged conjugated area of main ligands of these two complexes. Third, it is very important that all dihedral angles of main ligands of these two complexes are close to 0.0, or 180.0, showing that

TABLE-1
COMPUTATIONAL SELECTED BOND LENGTHS (NM), BOND ANGLES (º) AND DIHEDRAL ANGLES (º)
OF $[RU(BPY)_2(BOPP)]^{2+}$ **1**, $[RU(BPY)_2(DPPZ)]^{2+}$ **2** AND $[RU(BPY)_3]^{2+}$ 0 FOR COMPARISON

Comp.	Ru-N_m [a]	Ru-N_{co}	C-C$(N)_m$ [b]	C-C$(N)_{co}$	A_m [c]	A_{co}	Dihedral angle		
0 (calc)	0.2079	0.2079	0.1400	0.1400	78.4	78.4	–	–	–
$[Ru(bpy)_3]^{2+}$(expt)	0.2056	0.2056	0.1360	0.1360	78.7	78.7	–	–	–
1 (L = bopp)	0.2111	0.2098	0.1401	0.1400	79.2	78.4	2.0/176.9 (C1-C2-C3-O4) /(C1′-C2′-C3′-N6′)	-0.4/-175.3 (C5-C2-C3-N6) /(C5-C2-C3-N4)	174.0/-174.2 (C2-C3-C4-N7) /(C2′-C3-C6′-N8′)
2 (L = dppz)	0.2109	0.2097	0.1403	0.1400	79.1	78.5	180.0/180.0 (N1-C2-C3-C4) /(N5-C6′-C7′-C8′)	180.0/180.0 (N1-C2-N6-C7)/ (N5′-C6′-N2′-C3′)	0.0/0.0 (C2-C3-C4-C8) /(C6′-C7′-C8′C4′)

[a]Ru–N_m expresses the mean coordination bond length between Ru and N atoms of the main ligand (L = bopp), and Ru-N_{co} expresses that between Ru and N atoms of the co-ligand (bpy). [b]C-C$(N)_m$ expresses the mean bond length of ring skeleton of the main ligand, and C-C$(N)_{co}$ expresses that of the co-ligand. [c]A_m expresses the coordination bond angle between Ru and two N atoms of the main ligand, amd A_{co} expresses that of the co-ligand.

the planarities of main ligands of these two complexes are all very excellent and thus they must be easy to bind to DNA-base-pairs in intercalative mode. On the other hand, the main ligand (bopp) of complex **1** contains the N atoms with lone-pair electrons similar to the main ligand (dppz) of complex **2** and thus complex **1** has also the structural characteristic which can make the luminescence of the complex lose in aqueous solution. Therefore, based on these important structural characteristics of complex **1**, it can be prelimentorily expected to be an excellent DNA-light-switch complex. Further studies on the electronic structure and the DNA-binding and spectral properties of complex **1** are given below.

Electronic structures and related DNA-binding property: Besides of the geometric structure characteristics, the energies and populations of the frontier molecular orbitals of Ru(II) polypyridyl complexes are very important to design DNA-molecular light-switches, because the light-switches must exhibit not only a negligible background emission in water but also exhibit an intense luminescence in the presence of double strand DNA. For the first condition, as the above-mentioned, complex **1** has the structural characteristic making the complex non luminescence in water. Therefore, the present problem owes to the second condition which can make the complex exhibit an intense luminescence in the presence of double strand DNA. The intrinsic binding constants K_b of the complexes to calf thymus (CT) DNA have been measured by spectroscopic methods. It is observed that the DNA-binding constants (K_b) of the two complexes are K_b(**1**) of 2.4×10^6 and K_b(**2**) of 4.9×10^6, respectively[4,15], showing that both these two complexes have excellent DNA-binding properties and they can bind to DNA-base-pairs in intercalative mode. Such a common feature for these two complexes can be reasonably explained by the DFT calculations.

Many reports have shown the following points: (1) There are π-π stacking interactions in the DNA-binding of Ru(II) polypyridyl-type complexes in an intercalative (or partly intercalative) mode[3,41]. (2) DNA molecule is an electron-donor and an intercalated complex is an electron-acceptor[42-44]. (3) When the main ligand of complex parallelly intercalates DNA-pairs, the hydrophobic environment inside the DNA helix reduces the accessibility of water molecules to the complex leading to intense luminescence and the enlarged luminescence closely relates to the DNA-binding affinity of the complex[3,45-47]. (4) The trend in DNA-binding affinities of Ru(II) polypyridyl complexes theoretically relates to the energies and population of the lowest unoccupied molecular orbital and its nearby unoccupied orbitals LUMO + x (x: 0, 1, 2 …) of the complex[48-53]. The more negative or lower energies of the LUMO + x as well as their excellent population on the intercalative ligand are advantageous to the DNA-binding affinity[54-57].

The computed energies of some frontier molecular orbitals of complexes **1** and **2** in vacuum are shown in Table-2. The stereo contour graphs of the some frontier molecular orbitals of these two complexes in vacuum are also shown in Fig. 2, from which we can find that the stereo contour graphs of the two complexes are very similar. First, the components of the HOMO-1 and HOMO-2 of the two complexes are characterized by *d* orbitals of the metal atom. Second, the components of the LUMO + 2 of these two complexes are characterized by *p* orbitals of C and N atoms in main-ligand (L). Moreover, the stereo contour graphs of the some frontier molecular orbitals of complex **1** in aqueous solution (Fig. 3) further show that the components of the LUMO, LUMO + 1, LUMO + 2 and LUMO + 10 for complex **1** all mainly populated on the main-ligand. On the other hand, Table-2 showed that the LUMO + x (x: 0, 1, 2 …) energies of complex **1** are all negative and rather lower and that they are very similar to complex **2** as well-accepted DNA-molecular light-switch. For example, ε_{LUMO}(**1**) (-7.505 eV) ~ ε_{LUMO}(**2**) (-7.510 eV); in particular, for the LUMO + 2 on which the -components of the main-ligands of these two complexes are predominantly populated, ε_{LUMO+2}(**1**) (-7.294 eV) ~ ε_{LUMO+2}(**2**) (-7.339 eV) in vacuum. All of these show that complex **1** has excellent electronic structural characteristics similar to complex **2**, leading to the greatly enlarged luminescence of this complex in the presence of DNA.

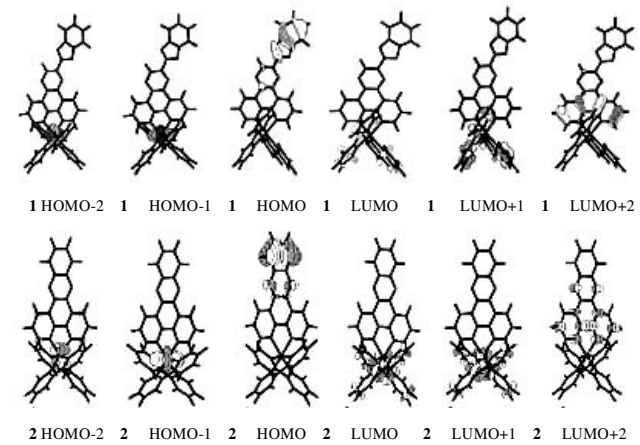

Fig. 2. Some related frontier MO contour plots of complex **1** and **2** in vaccum, based on the DFT-calculation

It is notable that our former work has shown that simply increasing the planar area of intercalative ligand may be ineffective on improvement of DNA-binding of resulting complex because of going with the increase in the LUMO (and LUMO+x) energy, but introducing some heteroatoms (*e.g.*, N atom) with stronger electronegativity into the ring skeleton of intercalative ligand should be effective because of

TABLE-2
ENERGIES (eV) OF SOME FRONTIER MOLECULAR ORBITALS OF COMPLEXES **1** AND **2** IN VACCUM USING THE DFT CALCULATION AT THE B3LYP/ LANL2DZ LEVEL

Compound	P. Group	HOMO-3	HOMO-2	HOMO-1	HOMO	LUMO	LUMO+1	LUMO+2
1	C_1	-11.005	-10.873	-10.298	-10.129	-7.505	-7.417	-7.294
2	C_2	1a	1b	2a	3a	2b	4a	3b
–	–	-10.990	-10.819	-10.870	-10.868	-7.510	-7.423	-7.339

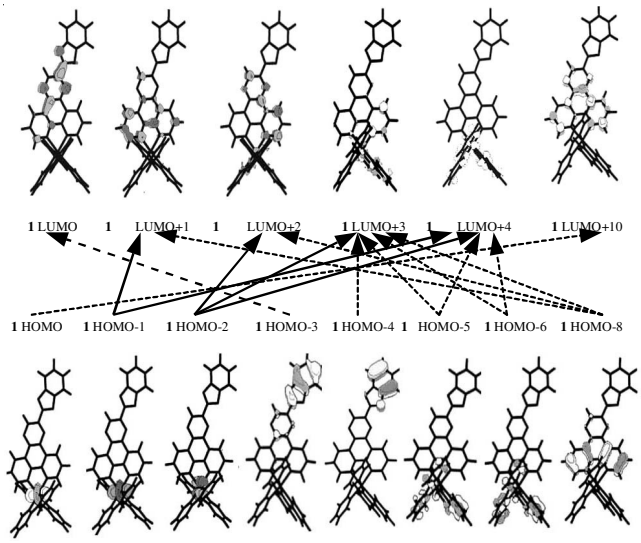

Fig. 3. Some related frontier MO contour plots of complex **1** in aqueous solution as well as the main transitions contributing to the experimental bands 448, 363 and 284 nm, respectively expressing by bold real line, broken line and point line allow-heads, based on the TDDFT-calculational results listed in Table-3

the decrease in the LUMO (and LUMO+x) energy to a certain extent[30]. Therefore, in the final analysis, that the complex **1** has the excellent electronic structural characteristics very similar to complex **2** should owe to the controlling action *via* introducing some heteroatoms (N and O atoms) with stronger electronegativity into the ring skeleton of main ligand.

Spectral simulation of the complex in aqueous solution and theoretical explanation: The electronic structure and related spectral properties of complex **1** in aqueous solution have further been computed by the TDDFT method at the B3LYP/LanL2DZ level. The stereo contour graphs of some frontier molecular orbitals of complex **1** in aqueous solution based on the TDDFT-calculation as well as the related orbital transitions for three strong bands of the electronic absorption-spectra are also shown in Fig. 3. Fig. 3 clearly shown the following facts: First, the components of the HOMO, HOMO-1 and HOMO-2 come mainly from *d* orbitals of the center metal atom (Ru) and thus these molecular orbitals can be characterized by *d* orbitals of the metal atom. Second, the components of the LUMO, LUMO+1, LUMO+2 and LUMO+10 come mainly from *p* orbitals of C and N atoms of main-ligand (L) and thus these molecular orbitals can be characterized by orbitals of main-ligand (L). Such component-characteristics of the frontier molecular orbitals can be easily used to explain the spectral properties of the complex.

The calculated absorption-spectral data, the related transfers and assignments of spectral bands, as well as the corresponding experimental data[15] of complex **1** are given in Table-3, considering the theoretical transitions characterized by an oscillator strength (f) larger than 0.10 and an orbital contribution larger than 10 % within 250-500 nm. The experimental electronic absorption spectra of complex **1** and their simulated ones in the range of 250-550 nm using the TDDFT method in aqueous solution are also shown in Fig. 4.

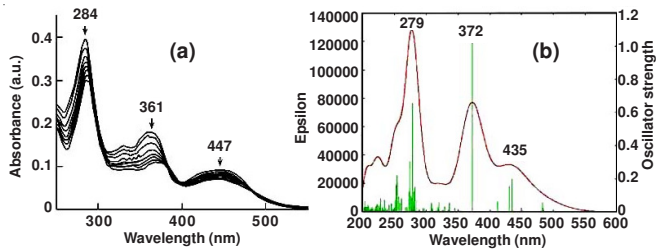

Fig. 4. Experimental electronic absorption spectra of complex **1** (a) and the simulated absorption spectra of complex **1**, based on the TDDFT-calculation in aqueous solution (b)

Fig. 4 showed that the simulated electronic absorption spectra of complex **1** in aqueous solution have three strong

TABLE 3
COMPUTED ABSORPTION SPECTRA AND THEIR ASSIGNMENTS OF $[RU(BPY)_2(BOPP)]^{2+}$ IN AQUEOUS SOLUTION USING THE TDDFT AT THE B3LYP/ LANL2DZ LEVEL AS WELL AS THE EXPERIMENTAL WAVELENGTHS (nm)

No	Wavelength (nm)			Assignments		
	Expt	Calcd.	f[a]			
1	448	435	0.198	HOMO-1 → LUMO+1 (29%)[b]	$d_{Ru}\rightarrow\pi^*_L$	^{1}MLCT
				HOMO-2 → LUMO+4 (25%)	$d_{Ru}\rightarrow\pi^*_{bpy}$	^{1}MLCT
		430	0.155	HOMO-2 → LUMO+3 (35%)	$d_{Ru}\rightarrow\pi^*_{bpy}+\pi^*_L$	^{1}MLCT
				HOMO-1 → LUMO+4 (32%)	$d_{Ru}\rightarrow\pi^*_{bpy}$	^{1}MLCT
				HOMO-2 → LUMO+2 (20%)	$d_{Ru}\rightarrow\pi^*_L$	^{1}MLCT
	363	372	1.029	HOMO-3 → LUMO (87%)	$\pi_L\rightarrow\pi^*_L$	^{1}LLCT
	284	282	0.147	HOMO-6 → LUMO+3 (16%)	$\pi_{bpy}\rightarrow\pi^*_{bpy}+\pi^*_L$	^{1}LLCT
				HOMO-8 → LUMO+1 (14%)	$\pi_L\rightarrow\pi^*_L$	^{1}LLCT
				HOMO-8 → LUMO+2 (12%)	$\pi_L\rightarrow\pi^*_L$	^{1}LLCT
		281	0.124	HOMO-6 → LUMO+4 (41%)	$\pi_{bpy}\rightarrow\pi^*_{bpy}$	^{1}LLCT
				HOMO-4 → LUMO+3 (11%)	$\pi_L\rightarrow\pi^*_{bpy}+\pi^*_L$	^{1}LLCT
				HOMO-5 → LUMO+3 (11%)	$\pi_{bpy}\rightarrow\pi^*_{bpy}+\pi^*_L$	^{1}LLCT
		279	0.655	HOMO-5 → LUMO+4 (29%)	$\pi_{bpy}\rightarrow\pi^*_{bpy}$	^{1}LLCT
				HOMO-6 → LUMO+3 (17%)	$\pi_{bpy}\rightarrow\pi^*_{bpy}+\pi^*_L$	^{1}LLCT
		274	0.306	HOMO-8 → LUMO+1 (22%)	$\pi_L\rightarrow\pi^*_L$	^{1}LLCT
				HOMO → LUMO+10 (18%)	$d_{Ru}\rightarrow\pi^*_L$	^{1}MLCT
				HOMO-8 → LUMO+3 (16%)	$\pi_L\rightarrow\pi^*_{bpy}+\pi^*_L$	^{1}LLCT

[a]Oscillator strength. [b]Percentage contributions to wavefunctions of excited states are given in parenthesis.

bands *ca*. 435, 372 and 279 nm. These three strong bands respectively correspond to the experimental three strong bands of *ca*. 448, 363 and 284 nm. The errors of the calculated wavelengths from experiment data for complex **1** in aqueous solution lie within 5-12 nm. The theoretical explanations for these simulated electronic absorption spectra are also carried out.

For the first strong lowest energy band (*ca*. 448 nm) in the experimental spectra of complex **1**, which is generally well-accepted ^{1}MLCT band, can be theoretically explained in as follows. From Table-3 and Fig. 3, we find that two calculated strong transitions with f > 0.15 lie in the range of 400-500 nm. The strongest band (f = 0.198) at 434.8 nm mainly involves the transition from HOMO-1- LUMO+1 (29 %) characterized by $d_{Ru} \rightarrow \pi^*_L$ and the other one from HOMO-2-LUMO+4 (25 %) characterized by $d_{Ru} \rightarrow \pi^*_{bpy}$. The next strongest band at 430.2 (f = 0.1551) nm has also an obvious ^{1}MLCT character and mainly involves the transition of HOMO-2 → LUMO+3 (35 %) characterized by $d_{Ru} \rightarrow \pi^*_{bpy}+\pi^*$ L and the transition of HOMO-1→ LUMO+4 (32 %) characterized by $d_{Ru} \rightarrow \pi^*_{bpy}$. Therefore, the experimental broad band of complex **1** at 448 nm can be assigned to a superposition of these two bands with ^{1}MLCT feature. Moreover, considering that the most important contribution to this experimental broad band is the transition from d_{Ru} (HOMO-1 or HOMO-2) to π^*_L (LUMO+1 or LUMO+2) and π^*_{bpy} (LUMO+3 or LUMO+4), the ^{1}MLCT band at 447 nm can be simply assigned to the transition of $d_{Ru} \rightarrow \pi^*_L$ and $d_{Ru} \rightarrow \pi^*_{bpy}$.

For the second strong band (*ca*. 363 nm) in the experimental spectra, from Table-3 and Fig. 3, we can clearly see that the calculated strong band at 372 nm with great oscillator strength (f = 1.029) has an obvious ^{1}LLCT character and mainly originates from HOMO-3 → LUMO (87 %) ($\pi_L \rightarrow \pi^*_L$). Therefore, the experimental broad band at 361 nm can be mainly assigned to this calculated band and can be characterized by the ^{1}LLCT transition with $\pi_L \rightarrow \pi^*_L$ feature.

For the third strong band (*ca*. 284 nm) in the experimental spectra, from Table-3 and Fig. 3, we find that four calculated strong bands (*ca*. 282.0, 280.6, 278.6 and 274.2 nm) are mainly involved in this simulated band. First, the band (f = 0.147) at 282 nm mainly involves the transition from π_{bpy} (HOMO-6) to π^*_{bpy} π^*_L (LUMO + 3) (16 %) and it can be characterized by $\pi_{bpy} \rightarrow \pi^*_{bpy}+\pi^*_L$. Besides this most contributing transition, this band also involves several transitions with the character of $\pi_L \rightarrow \pi^*_L$, *i.e*., HOMO-8 → LUMO+1 (14 %) and HOMO-8 → LUMO+2 (12 %). Next, the band (f = 0.124) at 280.6 nm mainly involves the transition from (HOMO-6) to (LUMO+4) (41 %), which can be characterized by $\pi_L \rightarrow \pi^*_L$ and also involves the other transitions HOMO-4 → LUMO+3 (11 %) and HOMO-5 → LUMO+3 (11 %) with the character of $\pi_L \rightarrow \pi^*_{bpy} + \pi^*_L$ and $\pi_{bpy} \rightarrow \pi^*_{bpy} + \pi^*_L$. Next again, the band at 278.6 nm (f = 0.655) has an obvious ^{1}LLCT character and mainly originates from HOMO-5 → LUMO + 4 (29 %) ($\pi_{bpy} \rightarrow \pi^*_{bpy}$) and HOMO-6→ LUMO +3 (17 %) ($\pi_{bpy} \rightarrow \pi^*_{bpy} + \pi^*_L$). Final, the band at 274.2 nm (f = 0.306) mainly involves the transitions from HOMO-8 to LUMO+1 (22 %) and LUMO+3 (16 %), which can be characterized by $\pi_L \rightarrow \pi^*_L$ and $\pi \rightarrow \pi^*_{bpy}+\pi^*_L$, as well as the transition from HOMO to LUMO +10 (18 %) with the character of $d_{Ru} \rightarrow \pi^*_L$. Therefore, the experimental band of *ca*. 284 nm can be assigned as a superposition band of four calculated strong bands (*ca*. 282.0, 280.6, 278.6 and 274.2 nm) and its band can also be mainly characterized by ^{1}LLCT band.

In summary, experimental three strong electronic absorption bands of complex **1** can be satisfactorily simulated and explained by the TDDFT computations.

Theoretical analysis on the spectral properties of the complex: From Table-3 and Fig. 3, it is very interesting to find the following points.

First, eight HOMO+x orbitals and six LUMO+x orbitals are the important orbitals in relation to the electronic transitions of complex **1** in the range of 250-550 nm, based on the TDDFT-calculations in aqueous solution.

Second, the LUMO+3 orbital is the most active electron-accepting orbital relating to five transitions from the HOMO-x to it; the LUMO+4 orbital is the most active electron-accepting orbital relating to four transitions; the LUMO+1 and LUMO+2 orbitals are also more active electron-accepting orbitals relating to the two transitions.

Third, the HOMO-2 and HOMO-8 are active electron-excited orbitals relating to the three transitions; the HOMO-1, HOMO-5 and HOMO-6 are also more active electron-excited orbitals relating to the two transitions.

Fourth, there are some strong transitions, *e.g*., HOMO-3 → LUMO, HOMO → LUMO+10 and HOMO-4 → LUMO+3, in relation to an excellent overlapping population of the related orbitals and an adjacent distance of the charge transfers.

In short, from the TDDFT calculations, we find that the related electron-excited and electron-accepting orbitals of every transition for the studied Ru(II) complex have an excellent overlapping population, in a good agreement with a general insight of the radiation theory[30,31,58]. Therefore, it further shows that the above computational results and spectral explanations are reliable.

Conclusion

The DFT study on the novel DNA-molecular light-switch complex $[Ru(bpy)_2(bopp)]^{2+}$ **1** shows that this complex has an excellent main ligand with a greater conjugated planar area as well as the lower LUMO+x (x: 0,1,2…) energies and the suitable populations of LUMO+x on the main ligand. Such geometric and electronic structural characteristics can finally owe to the controlling action *via* introducing some hetero-atoms (N and O atoms) with stronger electronegativity into the ring skeleton of main ligand. These important structural characteristics are advantageous to this complex firmly binding to DNA in interactive mode, leading to the greatly enlarged luminescence of the complex in the present of DNA, just as the well-accepted DNA-molecular light-switch complex $[Ru(bpy)_2(dppz)]^{2+}$ **2**. Meanwhile, the main ligand (bopp) of complex **1** has also the geometric structural characteristic, leading to nonluminescence of the complex in aqueous solution. Therefore, complex **1** can be expected to be a novel excellent DNA-light-switch complex. In particular, the electronic absorption spectra of complex **1** in aqueous solution were accurately calculated and simulated by the TDDFT method and the experimental three main UV-visible bands (*ca.* 448, 363 and 284 nm) were explained. Moreover, some regularities

regarding the strong electronic absorption spectra were also revealed, in a good agreement with the general insight of radiation theory.

ACKNOWLEDGEMENTS

The authors are pleased to thank the financial support of the National Natural Science Foundation of China (No. 20903026). Thanks are also due to the Information & Network Center, Sun Yat-Sen University for offering the High Performance Computing Clusters (HPCC).

REFERENCES

1. J.K. Barton, *Science*, **233**, 727 (1986).
2. T.-F. Miao, J. Li, Y.-T. Lu and K.-C. Zheng, *Asian J. Chem.*, **24**, 2891 (2012).
3. L.N. Ji, X.H. Zou and J.G. Liu, *Coord. Chem. Rev*., **513**, 216 (2001).
4. A.E. Friedman, J.C. Chambron, J.P. Sauvage, N.J. Turro and J.K. Barton, *J. Am. Chem. Soc*., **112**, 4960 (1990).
5. Y. Jenkins, A.E. Friedman, N.J. Turro and J.K. Barton, *Biochemistry*, **31**, 10809 (1992).
6. E. Ruba, J.R. Hart and J.K. Barton, *Inorg. Chem*., **43**, 4570 (2004).
7. E.J.C. Olsen, D. Hu, A. Hörmann, M.R. Arkin, E.D.A. Stemp, J.K. Barton and P.F. Barbara, *J. Am. Chem. Soc*., **119**, 11458 (1997).
8. C.G. Coates, J. Olofsson, M. Coletti, J.J. McGarvey, B. Onfelt, P. Lincoln, B. Norden, E. Tuite, P. Matousek and A.W. Parker, *J. Phys. Chem. B*, **105**, 12653 (2001).
9. I. Ortmans, B. Elias, J.M. Kelly, C. Moucheron and A. Kirsch-DeMesmaeker, *J. Chem. Soc., Dalton Trans*., 668 (2004).
10. M.J. Han, L.H. Gao, Y.Y. Lu and K.Z. Wang, *J. Phys. Chem. B*, **110**, 2364 (2006).
11. D. Kalinina, C. Dares, H. Kaluarachchi, P.G. Potvin and A.B.P. Lever, *Inorg. Chem*., **47**, 10110 (2008).
12. G.J. Wilson and G.D. Will, *Inorg. Chim. Acta*, **363**, 1627 (2010).
13. D. Ambrosek, P.F. Loos, X. Assfeld and C. Daniel, *J. Inorg. Biochem*., **104**, 893 (2010).
14. C.C. Ju, A.G. Zhang, C.L. Yuan, X.L. Zhao and K.Z. Wang, *J. Inorg. Biochem*., **105**, 317 (2011).
15. M.J. Han, Z.M. Duan, Q. Hao, S.Z. Zheng and K.Z. Wang, *J. Phys. Chem. C*, **111**, 16577 (2007).
16. Q. Hao, Z.M. Duan, M.J. Han, S.Z. Zheng, Y.Y. Lu and K.Z. Wang, *Chem. J. Chin. Univ.*, **27**, 1217 (2006).
17. D.A. Lutterman, A. Chouai, Y. Liu, Y.J. Sun, C.D. Stewart, K.R. Dunbar and C. Turro, *J. Am. Chem. Soc*., **130**, 1163 (2008).
18. I. Ciofini, P.P. Lainé, F. Bedioui and C. Adamo, *J. Am. Chem. Soc*., **126**, 10763 (2004).
19. D. Jacquemin, J. Preat, V. Wathelet, M. Fontaine and E.A. Perpète, *J. Am. Chem. Soc*., **128**, 2072 (2006).
20. B.D. Alexander, T.J. Dines and R.W. Longhurst, *J. Phys. Chem*., **352**, 19 (2008).
21. G. Pourtois, D. Beljonne, C. Moucheron, S. Schumm, A. Kirsch-De Mesmaeker, R. Lazzaroni and J.L. Brédas, *J. Am. Chem. Soc*., **126**, 683 (2004).
22. A. Dreuw, B.D. Dunietz and M. Head-Gordon, *J. Am. Chem. Soc*., **124**, 12070 (2002).
23. A. Dreuw and M. Head-Gordon, *J. Am. Chem. Soc*., **126**, 4007 (2004).
24. A. Dreuw and M. Head-Gordon, *Chem. Rev*., **105**, 4009 (2005).
25. D. Jacquemin, E.A. Perpète, G.E. Scuseria, I. Ciofini and C. Adamo, *J. Chem. Theory Comput*., **4**, 123 (2008).
26. A. Tsolakidis and E. Kaxiras, *J. Phys. Chem. A*, **109**, 2373 (2005).
27. S. Fantaccia, F. De Angelis, A. Sgamellotti and N. Re, *Chem. Phys. Lett*., **396**, 43 (2004).
28. S. Fantacci, F.D. Angelis, A. Sgamellotti, A. Marrone and N. Re, *J. Am. Chem. Soc*., **127**, 14144 (2005).
29. J. Li, L.C. Xu, J.C. Chen, K.C. Zheng and L.N. Ji, *J. Phys. Chem. A*, **110**, 8174 (2006).
30. J. Li, J.C. Chen, L.C. Xu, K.C. Zheng and L.N. Ji, *J. Organomet. Chem*., **692**, 831 (2007).
31. L.C. Xu, J. Li, Y. Shen, K.C. Zheng and L.N. Ji, *J. Phys. Chem. A*, **111**, 273 (2007).
32. L.C. Xu, J. Li, S. Shi, K.C. Zheng and L.N. Ji, *J. Mol. Struct. (Theochem)*, **855**, 77 (2008).
33. T.F. Miao, S.Y. Liao, L. Qian, K.C. Zheng and L.N. Ji, *Biophys. Chem*., **140**, 1 (2009).
34. P.J. Hay and W.R. Wadt, *J. Chem. Phys*., **82**, 270 (1985).
35. W.R. Wadt and P.J. Hay, *J. Chem. Phys*., **82**, 284 (1985).
36. V. Barone and M. Cossi, *J. Phys. Chem. A*, **102**, 1955 (1998).
37. M.J. Frisch, G.W. Trucks, H.B. Schlegel, G.E. Scuseria, M.A. Robb, J.R. Cheeseman, J.A. Montgomery Jr., T. Vreven, K.N. Kudin, J.C. Burant, J.M. Millam, S.S. Iyengar, J. Tomasi, V. Barone, B. Mennucci, M. Cossi, G. Scalmani, N. Rega, G.A. Petersson, H. Nakatsuji, M. Hada, M. Ehara, K. Toyota, R. Fukuda, J. Hasegawa, M. Ishida, T. Nakajima, Y. Honda, O. Kitao, H. Nakai, M. Klene, X. Li, J.E. Knox, H.P. Hratchian, J.B. Cross, V. Bakken, C. Adamo, J. Jaramillo, R. Gomperts, R.E. Stratmann, O. Yazyev, A.J. Austin, R. Cammi, C. Pomelli, J.W. Ochterski, P.Y. Ayala, K. Morokuma, G.A. Voth, P. Salvador, J.J. Dannenberg, V.G. Zakrzewski, S. Dapprich, A.D. Daniels, M.C. Strain, O. Farkas, D.K. Malick, A.D. Rabuck, K. Raghavachari, J.B. Foresman, J.V. Ortiz, Q. Cui, A.G. Baboul, S. Clifford, J. Cioslowski, B.B. Stefanov, G. Liu, A. Liashenko, P. Piskorz, I. Komaromi, R.L. Martin, D.J. Fox, T. Keith, M.A. Al-Laham, C.Y. Peng, A. Nanayakkara, M. Challacombe, P.M.W. Gill, B. Johnson, W. Chen, M.W. Wong, C. Gonzalez and J.A. Pople, Gaussian 03, Revision D.01; Gaussian, Inc.: Wallingford CT (2005).
38. M. Cossi, N. Rega, G. Scalmani and V. Barone, *J. Comp. Chem*., **24**, 669 (2003).
39. G. Schaftenaar, Molden V4.2, Program CAOS/CAMM Center Nijmegen Toernooiveld, Nijmegen, The Netherlands (1991).
40. K.C. Zheng, H. Deng, X.W. Liu, H. Li, H. Chao and L.N. Ji, *J. Mol. Struct. (Theochem.)*, **682**, 225 (2004).
41. X.H. Zou, B.H. Ye, H. Li, Q.L. Zhang, H. Cao, J.G. Liu, L.N. Ji and X.Y. Li, *J. Biol. Inorg. Chem*., **6**, 143 (2001).
42. D. Reha, M. Kabelác, F. Ryjácek, J. Šponer, J.E. Šponer, M. Elstner, S. Sándor and P. Hobza, *J. Am. Chem. Soc*., **124**, 3366 (2002).
43. N. Kurita and K. Kobayashi, *Comp. Chem*., **24**, 351 (2000).
44. K. Fukui, T. Yonezawa and H. Shingu, *J. Chem. Phys*., **20**, 722 (1952).
45. K.C. Zheng, J.P. Wang, W.L. Peng, X.W. Liu and F.C. Yun, *J. Phys. Chem. A*, **105**, 10899 (2001).
46. H. Xu, K.C. Zheng, H. Deng, L.J. Lin, Q.L. Zhang and L.N. Ji, *New J. Chem*., **27**, 1255 (2003).
47. X.W. Liu, J. Li, K.C. Zheng, H. Chao and L.N. Ji, *J. Inorg. Biochem*., **99**, 2372 (2005).
48. X.W. Liu, J. Li, H. Deng, K.C. Zheng, Z.W. Mao and L.N. Ji, *Inorg. Chim. Acta*, **358**, 3311 (2005).
49. S. Shi, J. Liu, J. Li, K.C. Zheng, C.P. Tan, L.M. Chen and L.N. Ji, *J. Chem. Soc. Dalton Trans*., 2038 (2005).
50. S. Shi, J. Liu, J. Li, K.C. Zheng, C.P. Tan, L.M. Chen and L.N. Ji, *J. Inorg. Biochem*,. **100**, 385 (2006).
51. L.C. Xu, S. Shi, J. Li, S.Y. Liao, K.C. Zheng and L.N. Ji, *J. Chem. Soc., Dalton Trans*., 291 (2008).
52. B.H. Yun, J.O. Kim, B.W. Lee, P. Lincoln, B. Norden, J. M. Kim and S.K. Kim, *J. Phys. Chem. B*, **107**, 9858 (2003).
53. W.J. Mei, J. Liu, K.C. Zheng, L.J. Lin, H. Chao, A.X. Li, F.C. Yun and L.N. Ji, *J. Chem. Soc. Dalton Trans*., 1352 (2003).
54. X.W. Liu, J. Li, K.C. Zheng, Z.W. Mao and L.N. Ji, *Inorg. Chim. Acta*, **358**, 3311 (2005).
55. W.J. Wu, J.C. Chen, K.C. Zheng and F.C. Yun, *Chin. J. Chem. Phys*., **18**, 936 (2005).
56. T.F. Miao, J. Li, S.Y. Liao, J. Mei, K.C. Zheng and L.N. Ji, *J. Mol. Struct. (Theochem.)*, **957**, 108 (2010).
57. T.F. Miao, J. Li, S.Y. Liao, K.C. Zheng and L.N. Ji, *J. Inorg. Biochem*., **363**, 3880 (2010).
58. J. Li, L.C. Xu, S.Y. Liao, K.C. Zheng and L.N. Ji, *J. Theor. Comp. Chem*., **7**, 1147 (2008).